

## Parametric amplification and noise squeezing in room temperature atomic vapors

Guarrera, Vera; Gartman, Rafal; Barontini, Giovanni; Bevilacqua, Giuseppe; Chalupczak, Witold

DOI:

[10.1103/PhysRevLett.123.033601](https://doi.org/10.1103/PhysRevLett.123.033601)

License:

None: All rights reserved

*Document Version*

Publisher's PDF, also known as Version of record

*Citation for published version (Harvard):*

Guarrera, V., Gartman, R., Barontini, G., Bevilacqua, G. & Chalupczak, W. 2019, 'Parametric amplification and noise squeezing in room temperature atomic vapors', *Physical Review Letters*, vol. 123, no. 3, 033601. <https://doi.org/10.1103/PhysRevLett.123.033601>

[Link to publication on Research at Birmingham portal](#)

### **Publisher Rights Statement:**

Checked for eligibility: 19/07/2019

Guarrera, V., Gartman, R., Bevilacqua, G., Barontini, G. and Chalupczak, W. (2019). Parametric Amplification and Noise Squeezing in Room Temperature Atomic Vapors. *Physical Review Letters*, 123(3). © 2019 American Physical Society. The final Version of Record can be found at: <https://doi.org/10.1103/PhysRevLett.123.033601>

### **General rights**

Unless a licence is specified above, all rights (including copyright and moral rights) in this document are retained by the authors and/or the copyright holders. The express permission of the copyright holder must be obtained for any use of this material other than for purposes permitted by law.

- Users may freely distribute the URL that is used to identify this publication.
- Users may download and/or print one copy of the publication from the University of Birmingham research portal for the purpose of private study or non-commercial research.
- User may use extracts from the document in line with the concept of 'fair dealing' under the Copyright, Designs and Patents Act 1988 (?)
- Users may not further distribute the material nor use it for the purposes of commercial gain.

Where a licence is displayed above, please note the terms and conditions of the licence govern your use of this document.

When citing, please reference the published version.

### **Take down policy**

While the University of Birmingham exercises care and attention in making items available there are rare occasions when an item has been uploaded in error or has been deemed to be commercially or otherwise sensitive.

If you believe that this is the case for this document, please contact [UBIRA@lists.bham.ac.uk](mailto:UBIRA@lists.bham.ac.uk) providing details and we will remove access to the work immediately and investigate.

## Parametric Amplification and Noise Squeezing in Room Temperature Atomic Vapors

V. Guarrera,<sup>1,2,\*</sup> R. Gartman,<sup>2</sup> G. Bevilacqua,<sup>3</sup> G. Barontini,<sup>1</sup> and W. Chalupczak<sup>2</sup>

<sup>1</sup>Midlands Ultracold Atom Research Centre, School of Physics and Astronomy, University of Birmingham, Edgbaston, Birmingham B15 2TT, United Kingdom

<sup>2</sup>National Physical Laboratory, Hampton Road, Teddington TW11 0LW, United Kingdom

<sup>3</sup>DIISM, Università di Siena, via Roma 56, 53100 Siena, Italy



(Received 28 February 2019; published 17 July 2019)

We report on the use of parametric excitation to coherently manipulate the collective spin state of an atomic vapor at room temperature. Signatures of the parametric excitation are detected in the ground-state spin evolution. These include the excitation spectrum of the atomic coherences, which contains resonances at frequencies characteristic of the parametric process. The amplitudes of the signal quadratures show amplification and attenuation, and their noise distribution is characterized by a strong asymmetry, similar to those observed in mechanical oscillators. The parametric excitation is produced by periodic modulation of the pumping beam, exploiting a Bell-Bloom-like technique widely used in atomic magnetometry. Notably, we find that the noise squeezing obtained by this technique enhances the signal-to-noise ratio of the measurements up to a factor of 10, and improves the performance of a Bell-Bloom magnetometer by a factor of 3.

DOI: [10.1103/PhysRevLett.123.033601](https://doi.org/10.1103/PhysRevLett.123.033601)

*Introduction.*—Parametric excitation provides an excellent tool for gaining control over signal amplitude and noise in oscillating systems. As it is a coherent process with phase-sensitive character, it can be used to generate squeezed states that are crucial for technological developments, including implementations of quantum technology. Proof-of-principle demonstrations of this effect have been achieved in a variety of different systems ranging from mechanical oscillators [1–5], to optical modes [6] and ultracold atoms [7]. Parametric excitation of an oscillator is obtained by periodically modulating one of the system parameters, such as the oscillator natural frequency  $\omega_0$  or the damping rate, at frequencies that are submultiples of  $2\omega_0$  [8]. The excitation occurs because of a distortion of the system orbits in the phase space, without involving any direct perturbation of the equilibrium position of the oscillator. As a result, the dynamic response of the system at  $\omega_0$  is enhanced. It also shows a characteristic phase dependence: while the quadrature of the motion in phase with the parametric modulation is amplified, the orthogonal (out-of-phase) quadrature is attenuated. Likewise, fluctuations of the two quadratures are modified. This technique can be exploited to reduce the uncertainty in the determination of the frequency of an oscillator [2], and to achieve noise reduction below classical (e.g., thermal or technical) [1] and standard quantum limits [7,9].

Here we demonstrate parametric amplification and noise squeezing in the collective atomic spin system realized by an ensemble of optically pumped room temperature atoms, which is a widely exploited platform for magnetometry [10], quantum information processing [11], and rotation

sensing [12]. We show that by using such parametric squeezing we can enhance the signal-to-noise ratio in a Bell-Bloom magnetometer by up to a factor of 10. To understand the working principle of our parametric effect, let us consider a collective atomic spin precessing around a dc magnetic field  $\mathbf{B} = B\hat{x}$  with natural (Larmor) frequency  $\omega_L = gB$ , where  $g$  is the gyromagnetic ratio of the atoms. This system can be mapped onto an harmonic oscillator with frequency  $\omega_0 = \omega_L$ , where the components of the oscillating spin  $\hat{F}_y$  and  $\hat{F}_z$  take the place of position  $\hat{X}$  and momentum  $\hat{P}$  of a mechanical oscillator [13]. Parametric amplification and squeezing might be achieved in atomic spin systems by periodic modulation of either  $\omega_L$ , via modulation of the magnetic field amplitude, or the damping rate  $\gamma$  of the Larmor precession. In this Letter, we investigate this latter case by modulating the damping rate via the intensity modulation of the pump beam in a Bell-Bloom magnetometer [14].

In contrast to the standard Bell-Bloom scheme, in the present work we use a relatively strong pump resonantly coupled to one of the atomic ground states of cesium atoms, as shown in Fig. 1. The pump term, in this case, can be written in the density matrix formalism as [15]

$$\begin{aligned} \Gamma(t) &= -L_R\{WW^\dagger, \rho\} + 2L_R W\rho_e W^\dagger + (\rho'_e)_{sp} \\ &= \Gamma_a + \Gamma_p\rho, \end{aligned} \quad (1)$$

where  $W = -E_0(t)\Pi\mathbf{d} \cdot \mathbf{e}^*\Pi_e$  ( $W^\dagger = E_0(t)\Pi_e\mathbf{d} \cdot \mathbf{e}\Pi$ ), with  $E_0(t)$  and  $\mathbf{e}$  the amplitude and polarization versor of the laser field, respectively, and  $\mathbf{d}$  the induced atomic dipole

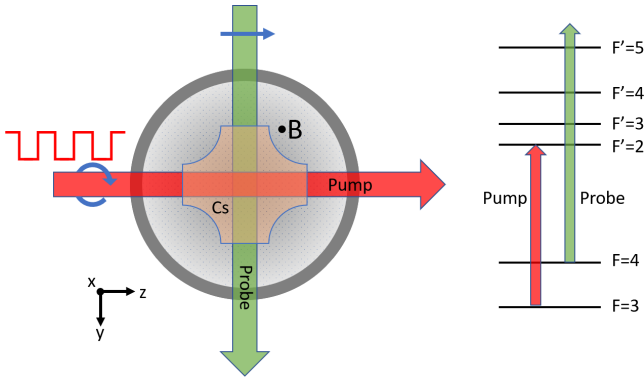


FIG. 1. Schematics of the apparatus: a circularly polarized amplitude-modulated pump beam creates atomic coherences in the ground states of the Cs atoms by resonant ( $F = 3$ ) and indirect pumping ( $F = 4$ ). The generated collective atomic spin precesses orthogonally to the applied static magnetic field. A linearly polarized probe beam is used to extract information on the atomic precession via Faraday-like, nondestructive measurements.

moment.  $\Pi$  and  $\Pi_e$  are the projectors on the ground and excited state (labeled with the letter  $e$ ) that are connected by the pump, and  $L_R$  depends on the natural linewidth of the transition. The first term in Eq. (1) accounts for depopulation of the ground-state, while the second and third refer to repopulation due to stimulated and spontaneous emission. In the dynamics of the macroscopic spin, the power broadening due to the pump beam contributes with a parametric term  $\Gamma_p$ , while the depopulation and repopulation due to stimulated and spontaneous emission are taken into account by an additive term  $\Gamma_a$ . The light shift induced by the pump is neglected in the condition of resonant pumping. We can write the evolution of the spin components of interest as

$$\begin{aligned} \frac{d^2 F_z}{dt^2} + [\gamma + \Gamma_p(t)] \frac{dF_z}{dt} + \omega_L^2 F_z - \omega_L \Gamma_a(t) &= 0, \\ \frac{dF_y}{dt} &= -\omega_L F_z, \end{aligned} \quad (2)$$

where  $\gamma = (1/T_2)$  is the rate of spin coherence relaxation due to spin-exchange collisions, and the pump is applied along the  $\hat{z}$  axis. Note that Eq. (2) describes the dynamics for the atoms in the directly pumped ground state. However, polarization and coherence generated by the pumping process in this state are also transferred to the other ground state primarily by spin-exchange interactions [15,16] and, secondarily, by off-resonant pumping. In our experiment, the delay in the dynamics of the two states due to the indirect pumping is smaller than the spin coherence relaxation time. Hence Eq. (2) is valid also for the atomic dynamics in the indirectly pumped ground state. This simplification of the model allows us to easily extract

useful information on the dynamical evolution of the atomic system.

From the equations above, it follows that in the presence of a modulated additive pump ( $\Gamma_p \ll \gamma$ ) coherent oscillation at the Larmor frequency has a transient character, while coherent oscillation at the modulation frequency  $\omega_M$  takes over in the stationary regime [17]. In other words, the pump acts on the collective spin system like a forcing term on a damped harmonic oscillator. For a relatively strong pump ( $\Gamma_p \gtrsim \gamma$ ), while these features remain generally valid, we have already observed that the coherence spectrum becomes more complex [15].

*Experimental setup.*—Details of the experimental configuration are described in Ref. [18] and here we only recall the key elements. As shown in Fig. 1, a cesium vapor is held in a paraffin coated, cross-shaped glass cell, placed within five layers of mu-metal shields. All measurements are performed with an atomic density of  $0.33 \times 10^{11} \text{ cm}^{-3}$ , at room temperature. The pumping is done by using a circularly polarized laser beam, frequency locked to the cesium  $6^2S_{1/2} F = 3 \rightarrow 6^2P_{3/2} F' = 2$  transition. The pump beam intensity is periodically switched on and off following a square modulation function. The signal produced by the  $F = 4$  ground-state atomic coherences is read out by a probe beam propagating along a direction orthogonal to the pump beam, frequency locked to the  $6^2S_{1/2} F = 4 \rightarrow 6^2P_{3/2} F' = 5$  transition, and subsequently frequency shifted by 960 MHz to the blue side. Probing the  $F = 4$  ground state allows us to decouple the effects of the pump and probe beams, while still capturing features of the atomic polarization dynamics of the directly pumped state. For our experimental parameters, the coherence from the  $F = 4$  atoms, following indirect pumping, is detectable already few tens ms after switching on the pump beam, with a peak amplitude around 80 ms [16]. These timescales are shorter than the coherence relaxation time,  $T_2 \sim 300$  ms. This is due to the coherence transfer hampering the SEC-induced decoherence process for degenerate Zeeman sublevel splitting [19] and, to a smaller extent, to off-resonant pumping to the  $F' = 3$  state (Doppler broadening is about 230 MHz).

A pair of Helmholtz coils produces a magnetic field orthogonal to the pump and probe beams. In this configuration, the continuous Faraday-type polarization rotation measurements provide information on the component of the collective spin parallel to the probe beam  $S(t) = k \langle F_y(t) \rangle$ , where  $k$  depends on the atomic transition used for probing and on the geometry of the magnetometer [20]. The probe light transmitted through the cell is analyzed by a polarimeter and processed by a signal analyzer or by a lock-in amplifier. This latter allows the extraction of  $(s_c, s_s)$  the spin projections in a frame rotating at frequency  $\omega_L$  which have slow fluctuations, i.e.,  $S(t) = s_c(t) \cos(\omega_L t) + s_s(t) \sin(\omega_L t)$ .

*Excitation spectrum.*—Figure 2(a) shows the excitation spectrum of the component at  $\omega_M$  in our configuration,

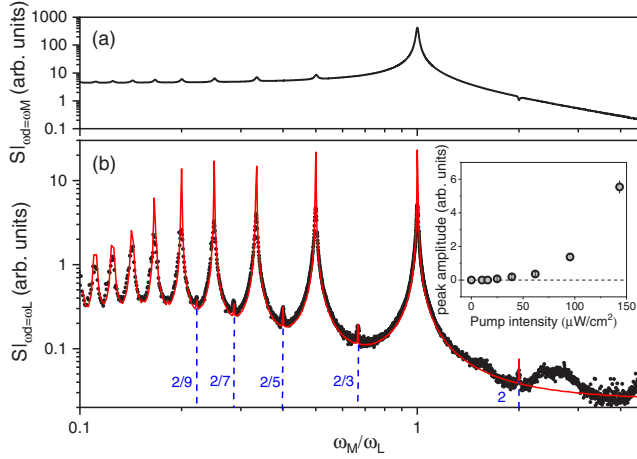


FIG. 2. Amplitude dependence of the  $F = 4$  atomic coherences oscillating at (a)  $\omega_M$ , and (b)  $\omega_L$  on the pump beam amplitude modulated at frequency  $\omega_M$ , recorded with a pump beam intensity of  $61 \mu\text{W}/\text{cm}^2$ . All measurements were made with a probe beam power of  $20 \mu\text{W}/\text{cm}^2$ , and  $\omega_L/2\pi = 270 \text{ Hz}$ . The solid red line represents the signal obtained by numerically solving Eq. (2). In the inset the amplitude of a parametric peak ( $\omega_M = 2/3\omega_L$ ) is shown as a function of the pump beam intensity.

which reveals the typical response of a harmonic oscillator driven by pulsed excitation. Since the amplitude of the pump beam is modulated with a square pulsed waveform, the spectrum of the optical excitation consists of a series of harmonics [17,18,21]. Up to this point, our system shows no difference with respect to a standard Bell-Bloom scheme.

To take a closer look at the dynamical response of the system, we extract the amplitude of the coherence signal oscillating at  $\omega_L$  from the FFT of the whole magneto-optical rotation signal. This amplitude is shown for different modulation frequencies in Fig. 2(b). We observe that, besides the usual Bell-Bloom resonances, a series of resonant features are visible at the characteristic frequencies of parametric amplification, i.e.,  $n\omega_M = 2\omega_L$ . On the basis of the above observations, these correspond to an enhancement of the detected signal oscillating at  $\omega_L$  that is not induced by pumping synchronization with the spin free evolution. The parametric peaks are visible for pump intensities above  $15 \mu\text{W}/\text{cm}^2$ , and their amplitude progressively increases for higher values of the pump, as shown in the inset of Fig. 2(b). We have also verified that they do not depend on the relative orientation of the probe beam and magnetic field for subtended angles between  $45^\circ$  and  $90^\circ$  [22].

We find good agreement between the experimental data and numerical simulations performed by solving Eq. (2), where  $\Gamma_p/\Gamma$  is kept as a free parameter, and  $\gamma$ ,  $\omega_L$ , and the time-averaged  $\Gamma_p$  are measured experimentally; see Fig. 2(b). We observe that the amplitude of the signal at modulation frequencies  $2/(2n+1)\omega_L$  is smaller than that at submultiples of  $\omega_L$ . This is due to the parametric amplification being

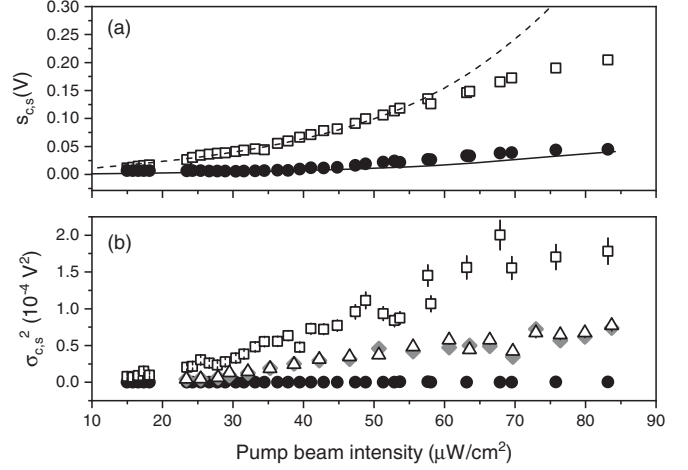


FIG. 3. (a) Amplitude of the in-phase (open squares) and out-of-phase (filled dots) components of the magneto-optical rotation signal oscillating at frequency  $\omega_L$  as a function of the pump beam intensity, with  $\omega_M = 2\omega_L$  and probe beam intensity of  $24 \mu\text{W}/\text{cm}^2$ . Solid lines are numerically calculated for the same parameters of Fig. 2(b). (b) Variance of the quadrature amplitudes over 350 measurements for the in-phase (open squares) and out-of-phase (filled dots) components as a function of the pump beam intensity. For comparison, the variance measured with a modulation frequency of  $4\omega_L$  is also reported (open triangles and gray diamonds).

effective only during the initial transient of the oscillation at  $\omega_L$ , when the system is not in an established autooscillating regime.

*Parametric amplification and squeezing at  $\omega_M = 2\omega_L$ .*— First, we concentrate our analysis on the behavior of the peak that appears in the spectrum for  $\omega_M = 2\omega_L$ . On the one hand, this allows us to address a characteristic parametric feature of the spectrum, on the other it allows us to single out the purely parametric effect as the natural frequency of the oscillation and the modulation frequency do not overlap. The amplitudes of the quadrature components ( $s_c, s_s$ ) in and out of phase with respect to the external modulation are extracted from the excitation spectrum measured 130 ms after the beginning of the pumping process, see Fig. 3(a). The lock-in amplifier used in these measurements is referenced to  $\frac{1}{2}\omega_M$ , while the Larmor frequency is scanned across the resonance  $\omega_L = \frac{1}{2}\omega_M$ . Figure 3(a) shows the dependence of the amplitude of the two signal quadratures on the pump beam intensity. Unlike nonparametric excitation, for which increasing the pump beam intensity below saturation leads to enhancement of overall polarization of the atomic system with the two quadratures growing by the same amount, here we observe that the in-phase and out-of-phase components grow at very different rates. In particular, the out-of-phase (in-phase) signal component is attenuated (amplified) by the parametric excitation with respect to the overall polarization growth. This can be understood by analytically

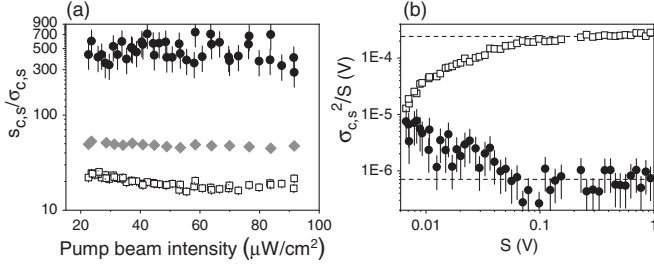


FIG. 4. (a) Signal-to-noise ratio of the signal quadratures measured for  $\omega_M = 2\omega_L$  as a function of the pump beam intensity. The out-of-phase quadrature (closed dots) shows an improved SNR with respect to the in-phase quadrature (open squares), and to the case of no modulation (gray diamonds). (b) Corresponding noise scaling with signal amplitude.

solving the dynamics for the quadrature components for a simple sinusoidal modulation of the pump. One obtains  $s_s(t) = s_0 e^{-(\gamma/2)t} e^{-(\Gamma_p/4)t}$  and  $s_c(t) = s_0 e^{-(\gamma/2)t} e^{(\Gamma_p/4)t}$ , where  $s_0$  is the maximum atomic polarization amplitude, also a function of the pump beam intensity. Comparison with numerical solutions of Eq. (2) provides good agreement for pump intensities up to roughly  $55 \mu\text{W}/\text{cm}^2$ . In fact, our simple model does not take into account other contributions that become more important for higher pump intensities, such as those from Stark-shift and saturation effects of the pump. Among the latter, we mention that off-resonant pumping can drive a net transfer of atoms from  $F = 3$  to  $F = 4$  which, by depleting the directly pumped level, hampers the indirect pumping process. For the highest pump beam intensities used, we observed this happening on the longer timescales of the steady state dynamics (few seconds from starting of the pump).

The effect of the parametric amplification on the two quadratures is also reflected in the behavior of the relative noise components. We observe that with increasing pump intensities, the noise is strongly squeezed along the attenuated quadrature and expanded along the other, see Fig. 3(b), leading to an asymmetric noise distribution. For comparison, in Fig. 3(b) we also show the measurement of the quadratures' noise for the nonparametric  $\omega_M = 4\omega_L$ . One can see that in the latter case the noise is equally distributed between the two quadratures.

Amplitude fluctuations are important as they affect the determination of the natural frequency of an oscillator in the presence of noise, and reduce the precision of magnetic field measurements. To evaluate this parameter we plot in Fig. 4(a) the signal-to-noise ratio (SNR) obtained by processing the polarization rotation signal with the lock-in amplifier as a function of the pump intensity for modulation frequency  $2\omega_L$ . The out-of-phase component (filled dots) shows an increased SNR with respect to the in-phase component (open squares) and, most importantly, to any component in the absence of modulation of  $\gamma$  (gray diamonds). Notably, with respect to this latter case the SNR

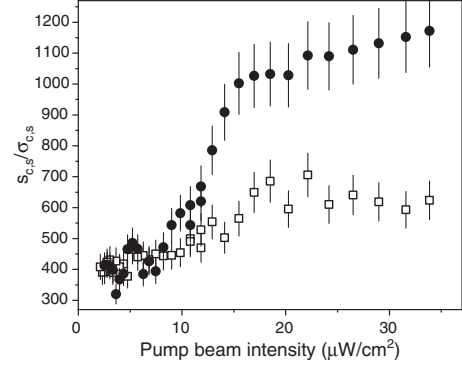


FIG. 5. Signal-to-noise ratio of a Bell-Bloom magnetometer, as a function of the pump beam intensity. Similar to the case of modulation at  $2\omega_L$ , the out-of-phase quadrature (closed dots) is increased with respect to the in-phase quadrature (open squares) for intensities larger than roughly  $15 \mu\text{W}/\text{cm}^2$ . Note that, as expected, the overall magnetization is higher when hitting the Bell-Bloom resonance with respect to other modulation frequencies.

enhancement is of 10 dB. We further analyze the noise scaling with the signal amplitude as shown in Fig. 4(b). At lower signal amplitudes, corresponding to pump intensities smaller than roughly  $50 \mu\text{W}/\text{cm}^2$ , the noise of the amplified (attenuated) component scales faster (slower) than linear. A fit with a function  $\sigma = as^b$  to the measured data yields  $b = 1.52(3)$  and  $b = 0.44(6)$ , respectively. A linear scaling, consistent with projection-noise-limited measurements, appears for higher signal amplitudes, concurrently with the deviation from the parametric behavior observed in Fig. 3(a). This suggests that the hampering of the parametric effect for larger pump beam intensities sets a major limitation to the maximum achievable squeezing.

*Enhanced Bell-Bloom magnetometer.*—Having analyzed the main features of the parametric excitation, we now show how such excitation improves the performance of a Bell-Bloom magnetometer beyond atomic projection noise. To this end, we report in Fig. 5 the SNR measured at  $\omega_M = \omega_L$  as a function of the pump beam intensity. To isolate the signal of the coherent oscillation at the Larmor frequency from the oscillation of the pump, the measurements are performed during the transient dynamics, when the former is dominant. We observe that with a pump beam intensity of  $36 \mu\text{W}/\text{cm}^2$  the SNR of our magnetometer is improved by a factor of 3. We attribute the reduced enhancement with respect to the case at  $2\omega_L$  to the presence of residual noise introduced by the pump which cannot be filtered out in the FFT of the signal. Nonetheless, our measurements reveal that the parametric noise squeezing obtained in the attenuated quadrature is a very robust technique for reducing the noise and improving SNR independently of our system being limited by atomic projection noise (for the case  $\omega_M = 2\omega_L$ ) or technical noise (for the case  $\omega_M = \omega_L$ ), as the method is fully classical and does not rely on the quantum features of the system. Currently, our system's

performance in the absence of the parametric effect for  $\omega_M = \omega_L$  and at low frequencies is mostly affected by Johnson noise of the magnetic shields at a level of  $50 \text{ fT}/\sqrt{\text{Hz}}$ . The presented technique allows an improvement in atomic noise to roughly  $15 \text{ fT}/\sqrt{\text{Hz}}$ . By redesigning the magnetic shielding of our experiment, we estimate that we can reduce technical noise below the level of  $10 \text{ fT}/\sqrt{\text{Hz}}$ , and in this case parametric squeezing could potentially bring the sensitivity below the  $1 \text{ fT}/\sqrt{\text{Hz}}$  level [23]. We finally note that the continuous measurement performed on the atomic system has minimal impact on the noise distribution. At the parametric resonances, we find that the degree of asymmetry in the noise distribution weakly depends on the probe beam intensity, and increases by roughly 10% when the power is raised from 20 to 500  $\mu\text{W}$  while the noise axis orientation does not significantly change in this range.

*Conclusions.*—In conclusion, signatures of parametric amplification and noise squeezing have been detected in the coherences of an optically pumped Cs vapor magnetometer. We have also shown that the signal-to-noise ratio can be increased up to a factor of 10 when the modulation frequency hits a parametric resonance and that the performance of a Bell-Bloom magnetometer can be enhanced by a factor of 3. Moreover, the system can be eventually led into a self-oscillating regime, which might be used to increase the measurement interrogation time beyond its natural decoherence and measurement bandwidth. Finally, we foresee application for noise control in combination with nondemolition measurements, as already explored in mechanical systems, for the “bright” squeezing generation [5].

The work was funded by the UK Department for Business, Innovation and Skills as part of the National Measurement System Programme. V. G. was supported by the EPSRC (Grant No. EP/S000992/1). We would like to thank R. Hendricks for critical reading of the manuscript.

---

\*v.guarrera@bham.ac.uk

- [1] D. Rugar and P. Grutter, *Phys. Rev. Lett.* **67**, 699 (1991).  
 [2] F. DiFilippo, V. Natarajan, K. R. Boyce, and D. E. Pritchard, *Phys. Rev. Lett.* **68**, 2859 (1992).

- [3] G. I. Harris, D. L. McAuslan, T. M. Stace, A. C. Doherty, and W. P. Bowen, *Phys. Rev. Lett.* **111**, 103603 (2013).  
 [4] A. Szorkovszky, A. C. Doherty, G. I. Harris, and W. P. Bowen, *Phys. Rev. Lett.* **107**, 213603 (2011).  
 [5] A. Pontin, M. Bonaldi, A. Borrielli, F. S. Cataliotti, F. Marino, G. A. Prodi, E. Serra, and F. Marin, *Phys. Rev. Lett.* **112**, 023601 (2014).  
 [6] R. E. Slusher, L. W. Hollberg, B. Yurke, J. C. Mertz, and J. F. Valley, *Phys. Rev. Lett.* **55**, 2409 (1985).  
 [7] T. M. Hoang, M. Anquez, B. A. Robbins, X. Y. Yang, B. J. Land, C. D. Hamley, and M. S. Chapman, *Nat. Commun.* **7**, 11233 (2016).  
 [8] L. Landau and E. Lifshitz, *Mechanics*, 3rd ed. (Butterworth-Heinemann, Oxford, 1976).  
 [9] E. E. Wollman, C. U. Lei, A. J. Weinstein, J. Suh, A. Kronwald, F. Marquardt, A. A. Clerk, and K. C. Schwab, *Science* **349**, 952 (2015).  
 [10] J. C. Allred, R. N. Lyman, T. W. Kornack, and M. V. Romalis, *Phys. Rev. Lett.* **89**, 130801 (2002).  
 [11] B. Julsgaard, J. Sherson, J. I. Cirac, J. Fiurasek, and E. S. Polzik, *Nature (London)* **432**, 482 (2004).  
 [12] M. E. Limes, D. Sheng, and M. V. Romalis, *Phys. Rev. Lett.* **120**, 033401 (2018).  
 [13] G. Vasilakis, H. Shen, K. Jensen, M. Balabas, D. Salart, B. Chen, and E. S. Polzik, *Nat. Phys.* **11**, 389 (2015).  
 [14] W. Bell and A. Bloom, *Phys. Rev. Lett.* **6**, 280 (1961).  
 [15] R. Gartman, V. Guarrera, G. Bevilacqua, and W. Chalupczak, *Phys. Rev. A* **98**, 061401(R) (2018).  
 [16] W. Chalupczak, P. Josephs-Franks, R. M. Godun, and S. Pustelny, *Phys. Rev. A* **88**, 052508 (2013).  
 [17] Z. D. Grujic and A. Weis, *Phys. Rev. A* **88**, 012508 (2013).  
 [18] R. Gartman and W. Chalupczak, *Phys. Rev. A* **91**, 053419 (2015).  
 [19] W. Chalupczak, P. Josephs-Franks, B. Patton, and S. Pustelny, *Phys. Rev. A* **90**, 042509 (2014).  
 [20] Y. Takahashi, K. Honda, N. Tanaka, K. Toyoda, K. Ishikawa, and T. Yabuzaki, *Phys. Rev. A* **60**, 4974 (1999).  
 [21] A small feature is also visible at  $2\omega_L$ , which is associated with alignment produced by the pump beam for higher pump powers, see D. Budker and D. F. Jackson Kimball, *Optical Magnetometry* (Cambridge University Press, Cambridge, England, 2013).  
 [22] We detect also a few broad features for modulation frequencies higher than  $2\omega_L$ , which have no direct impact on the present study and will be addressed in a separate paper.  
 [23] W. Chalupczak, R. M. Godun, S. Pustelny, and W. Gawlik, *Appl. Phys. Lett.* **100**, 242401 (2012).